Mathematical Biosciences and Engineering

Research article

Aqueous monitoring of toxic mercury through a rhodamine-based fluorescent sensor

Tahir Rasheed[1], Faran Nabeel[1], Muhammad Bilal[2,]*, Yuping Zhao[2], Muhammad Adeel[1] and Hafiz. M. N. Iqbal[3,]*

[1] School of Chemistry & Chemical Engineering, State Key Laboratory of Metal Matrix Composites, Shanghai Jiao Tong University, 800 Dongchuan Road, Shanghai, 200240, China

[2] School of Life Science and Food Engineering, Huaiyin Institute of Technology, Huaian 223003, China

[3] Tecnologico de Monterrey, School of Engineering and Sciences, Campus Monterrey, Ave. Eugenio Garza Sada 2501, Monterrey, N.L., CP 64849, Mexico

* **Correspondence:** Email: bilaluaf@hotmail.com, hafiz.iqbal@itesm.mx; Tel: +52(81)83582000 Ext. 5679.

Abstract: Mercury is a toxic heavy element, which contaminates air, land, and water, thus posing environment and human health-related threats to the ecological system. Considering the adverse ecological effects, there is an urgent need to design and develop strategic tools to detect a broader spectrum of toxic elements in different environments. The development of point-of-care tools, e.g., sensor-based devices offers a noteworthy solution to detect and monitor real-time generation or release of environmentally-related toxic elements from different sectors, even with or without partial treatments. For a first-hand estimate, a qualitative method (colorimetric) for detection of mercury could suffice. Benefiting from the colorimetric recognition methodology, herein, we developed a new system (2-(5-bromothiazol-2-yl)-3',6'-bis(diethylamino)spiro[isoindoline-1,9' xanthen]-3-one) for the detection of mercury ions. The newly developed chemical sensor is composed of a fluorescent part (rhodamine b) and a binding site (2-amino-5-bromothiazole). A highly selective and sensitive response accompanied by visual color change (colorless to pink) towards Hg^{2+} was observed among miscellaneous metal cations. This colorimetric change confirmed that the coordination complex exists as spirocyclic ring opened derivative of rhodamine moiety. Furthermore, the binding affinity and detection limit was also calculated from the absorbance and emission data. The calculated values are in the order of 4.72×10^4 M^{-1} and 6.9 μM, respectively. In addition, the results reveal that the complex between the chemical sensor (S) and Hg^{2+} is reversible in the presence of

ethylenediaminetetraacetate (EDTA^{2-}). Finally, the newly developed sensor S was employed to detect Hg^{2+} in the wastewater. The fluorescence intensity was measured at 583 nm with S followed by spiking with Hg^{2+} at different concentrations and related linearly. In summary, taken together all the properties suggest that the newly developed sensor might display great potential in the field of environmental monitoring of toxic elements.

Keywords: toxic mercury; rhodamine; colorimetric; high sensitivity; reversible

1. Introduction

In recent years, fluorescent visual detection of metal ions has been regularly used due to highly sensitive, selective, cost-effective and operational simplicity [1–5]. Conventional approaches such as electrochemical sensors inductively coupled plasma mass, and atomic absorption-emission spectrometry are considered laborious, time-consuming and complex procedures [6,7]. Despite their high selectivity and sensitivity to detect the total amount of the metal analytes [8], still, these do not fit in the list of real-time detection and evaluation methods [9]. Therefore, simple, low-cost, and convenient approaches are needed for real-time recognition of metal ions. Recently reported probes and various types of biosensors are important owing to their highly selective and sensitive detection of toxic heavy metal ions and other environmentally-related contaminants [3–5,10–12]. Thus, many of such bio-sensing tools are widely used for medical and environmental monitoring applications [12–16].

Excessive use of heavy metals for industrial applications has become a serious environmental concern for the last two decades [17,18]. Mercury is a highly toxic metal and is found in the atmosphere, land, and water [19]. Methyl-mercury, a derivative of mercury produced by microbial interaction, is even more lethal and can damage the intestine, lungs, kidney, heart nervous system and DNA causing Minamata and brain diseases following entrance into the body [14,20,21]. Based on its toxicity, international organizations such as the Environmental Protection Agency (EPA) and World health organization (WHO) have devised permissible mercury values for drinking water [22]. Hence, the development of sensitive and selective methods is highly essential for consistent monitoring and effective control of mercury-based environmental pollution.

Mercury fluorescent chemo-sensors consist of various active moieties known as fluorophores such as xanthenes (rhodamines and fluorescein), dansyl, pyrene and 1, 8-naphthalamide [9,23–26]. Rhodamine-based fluorescent chemosensors have greater photostable properties of molar extinction-coefficient (ε), long emission and absorption wavelengths, excellent spirolactam configuration, enhanced quantum yield (Φ) and visual detection through turn-on fluorescence [27,28]. Rhodamine-based fluorescent chemosensors, both in open cycle (fluorescent) and spirocyclic ring (colorless) form, have been developed for the recognition of heavy metals [29,30]. Reports have shown that oxygen and nitrogen at the binding location have an excellent affinity for mercury metal ions [4,5,31].

The present study aimed to develop a mercury metal ion rhodamine-based fluorescent chemosensor with enhanced sensitivity and selectivity assuming that the prepared sensor could be cost-effective and simple operative for real-time in-field investigation purposes. Scheme 1 illustrates a synthetic route of the desired chemical sensor (S) synthesized from rhodamine as a fluorophore. The characteristic structure of the newly developed chemosensor was confirmed by ^{1}H NMR and

mass spectroscopy. The colorless, nonfluorescent, rhodamine-based chemosensor when interacting with mercury metal ions changes to highly fluorescent pink color through spirolactam ring opening by chemical coordination interactions [32]. This characteristic property could be used for sensitive and selective monitoring of mercury metal ions as a mobile probe and color matching kit by observing molar extinction coefficient values against the concentration of mercury ions in the test sample.
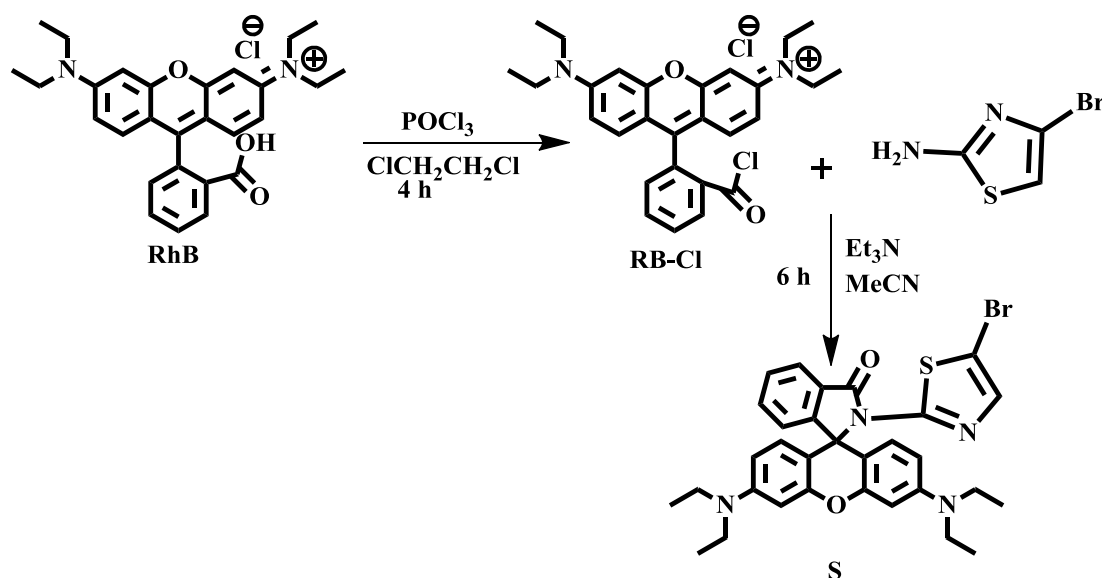
Scheme 1. A synthetic pathway for chemosensor development.

2. Materials and methods

2.1. Reagents and instrumentation

All the chemical or reagents were mainly purchased from Sigma-Aldrich USA, Adamas-Beta, and Shanghai Chemical Reagent Co. Ltd., China, and used as received. The solutions for different metal cations were prepared from their nitrates, chloride and perchlorate salts. PerkinElmer LS 55 and UV-Schimadzu 2600 spectrophotometer were used for fluorescence and UV-Vis measurements, respectively. For ^{1}H, ^{13}C and Mass analysis, mercury plus 400 spectrometer (Varian, USA) and Instrument: Waters ACQUITY UPLC & Micromass Q-TOF Premier Mass Spectrometer was used.

2.2. Development of rhodamine-based fluorescent sensor

A rhodamine-based fluorescent sensor was developed using rhodamine B acid chloride (RB-Cl) by adopting an earlier described process with slight modifications [33]. Briefly, 2.0 g of 4.2 mM phosphorous oxychloride in dichloroethane (DCE) was dropwise added to rhodamine B solution under continuous stirring and finally refluxing the solution for four h. The resultant reaction mixture was then cooled down to room temperature, and the solvent was eliminated under reduced pressure to obtain a purple sticky solid (RB-Cl). The collected RB-CI was thawed in 20 mL of anhydrous CH₃CN at room temperature. Following that, up to 20 mL mixture comprised on five mL of

anhydrous trimethylamine and 1.4 g (8.4 mM) 2-aminothiazole in acetonitrile was added dropwise using an ice bath. After cooling down to room temperature; the mixture was poured into 100 mL of distilled water, extracted with DCM and dried over anhydrous Na_2SO_4. The organic layer was evaporated, and the crude product was separated by column chromatography using 9:1 (v/v) DCM/CH$_3$OH as an eluent. The formation of S was confirmed by ^{1}H NMR and mass spectrometry (Figure 1).
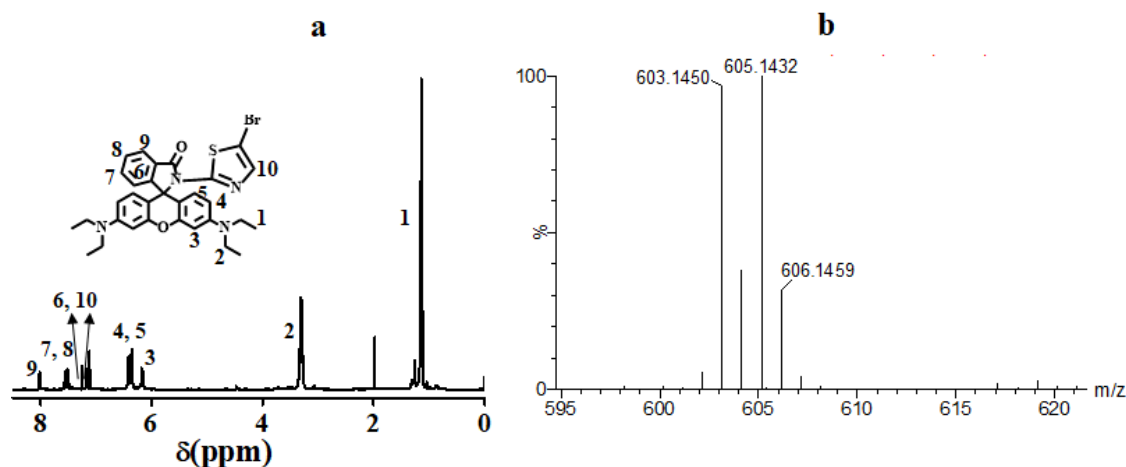

Figure 1. (a) ^{1}H NMR spectra in CDCl$_3$ and (b) MS spectra of S.

2.3. Sample preparation for aqueous monitoring of mercury

Initially, all the stock solutions were prepared using deionized water at a concentration of 100 mM. For mercury detection, up to 10 mL of acetonitrile was used to prepare the stock solution of sensor S with a final concentration of 100 mM. All freshly prepared stock solutions were further diluted to the desired concentration by adding the required amount of water. The spectral investigations were carried out in MeCN/H$_2$O (8:2 v/v) mixed solution. The samples were excited at a wavelength of λ_{max} = 550 nm, accompanied by excitation and emission slit width of = 15.0 nm. Similarly, the UV-Visible experiments were carried out within a wavelength of 400–700 nm in a quartz cuvette.

2.4. Binding constant calculation

The fluorescence and UV-Vis responses of S towards different metal cations were measured in CH$_3$OH: H$_2$O (8:2 v/v) at 583 and 559 nm, using 10 μM of S. The emission and absorbance intensities were fitted to Benesi-Hildebrand equations (1 and 2).

$$\frac{1}{\Delta(A-A_0)} = \frac{1}{K_a(A_{max}-A_0)[Cu^{2+}]} + \frac{1}{(A_{max}-A_0)} \tag{1}$$

$$\frac{1}{\Delta(F-F_0)} = \frac{1}{K_a(F_{max}-F_0)[Hg^{2+}]} + \frac{1}{(F_{max}-F_0)} \tag{2}$$

Where A/F and A_0/F_0 is absorbance/emission intensity of the **S** solution in the existence of Hg^{2+};

A_{max}/F_{max} is the saturated absorbance/emission in case of much more presence of Hg^{2+}; concentration of the mercury ion is presented as $[Hg^{2+}]$. Binding constants was "K_a" calculated from UV-visible records for Hg^{2+}.

2.5. Computational studies

The geometries of S and S-Hg^{2+} were determined by using density functional theory (DFT) calculations with the hybrid-generalized gradient approximation (HGGA) functional B3LYP. The effective core potential LanL2DZ basis and binary valence 3–21g basis set were allocated to (C, N, H, O, and Br) and metallic elements respectively, which have been proved an effective method for investigating the luminous mechanism of fluorescence probe. The Gaussian09 program package was for these calculations [34,35].

2.6. Real-time monitoring of Hg^{2+} in the contaminated wastewater

The practical applicability of the chemical sensor S was determined by measuring Hg^{2+} in wastewater samples. The contaminated wastewater samples were collected from the industrial area of Shanghai, China. Prior to measurements, following pH adjustment to neutral using phosphate buffer, the neutralized wastewater samples with a 20 mL working volume were passed through the microfiltration membranes. Different aliquots of the test samples were spiked with different concentrations, i.e., 0.1, 0.2, 0.4, 0.6, 0.8, 1.0 μM of freshly prepared mercury solution. The resulting samples were further treated with sensor S to give the final mixture (2.0 mL) containing S with final concentration of 10 μM and mercury (0.1, 0.2, 0.4, 0.6, 0.8, 1.0 μM) for 10 min at room temperature, and the absorbance was measured. The results were reported as the mean ± standard deviation of triplicate experiments for mercury and shown in Table 1.

Table 1. Determination of Hg^{2+} ions in industrial wastewater.

Sample	Hg^{2+} spiked (μM)	Hg^{2+} recovered (μM)	Recovery (%)
	0.0	Not detected	Not detected
	0.2	0.221 ±0.010	110.5
	0.4	0.398 ±0.014	99.5
Industrial wastewater	0.6	0.625 ±0.036	104.1
	0.8	0.824 ±0.006	103
	1.0	0.996 ±0.017	99.6

3. Results and discussion

3.1. Spectral investigations in the presence of Hg^{2+}

The spectral investigations (UV-Vis and fluorescence) of the newly fabricated chemical sensor S were carried out by titration experiments in acetonitrile: water system (8:2 v/v). The blank solution of S (10 μM) shows no significant enhancement of fluorescence as well as absorption intensities at 583 nm and 558 nm, respectively.

This turn-off response shows that the chemical sensor S exists in its ring-closed form. However,

upon the introduction of Hg^{2+}, a new emission peak at 583 nm appeared, the intensity of the emission band goes on increasing as the concentration of Hg^{2+} was increased from 0 to 40 μM. Also, the color of the solution changes from colorless to pink. This colorimetric change accompanied by the increased intensity value reveals that the sensor S exists in its ring-open form. This colorimetric change proves that the sensor S can serve as a bare-eye detector for Hg^{2+}. Similarly, the sensitive nature of the S was investigated by treating 10 μM solution of perchlorates, chlorides and nitrate solutions of different metal cations such as, Ag^+, Al^{3+}, Ba^{2+}, Ca^{2+}, Cd^{2+}, Fe^{3+}, Fe^{2+}, K^+, Li^+, Mg^{2+}, Mn^{2+}, Cu^{2+}, Pb^{2+}, Ni^+, Na^+ and Zn^{2+}. In CH_3OH: H_2O (8:2 v/v). Among all the competitive metal cations, only Hg^{2+} causes a significant change in the spectral pattern of S (Figure 2a, 2b). The binding affinity of the chemical sensor S was evaluated by using the emission titration data (Figure 3a). As shown in Figure 3b, the emission intensity increases to a certain value when the concentration of S and Hg^{2+} is equal to 1 equivalent. After that, the increase in intensity attains equilibrium.

Further, the binding stoichiometry was calculated by the method of continuous variables. During the process, the overall concentration of S and analyte remains constant (10 μM). After plotting the mole fraction of concentrations of S and analyte against corresponding intensity values, it was found that the binding stoichiometry of the complex S-Hg^{2+} was equal to 1:1 (Figure 3c). Finally, the equation 1 and 2 given in material method section was used to calculate the binding constant of the complex S-Hg^{2+}. The calculated value was equal to $4.72 \times 10^4 \, M^{-1}$. Similarly, the UV-Vis titration experiments were also carried out. The binding stoichiometry and binding constant calculated from UV-Vis titration data were in good agreement with the results obtained from emission titration experiments (Figure 3d–f).
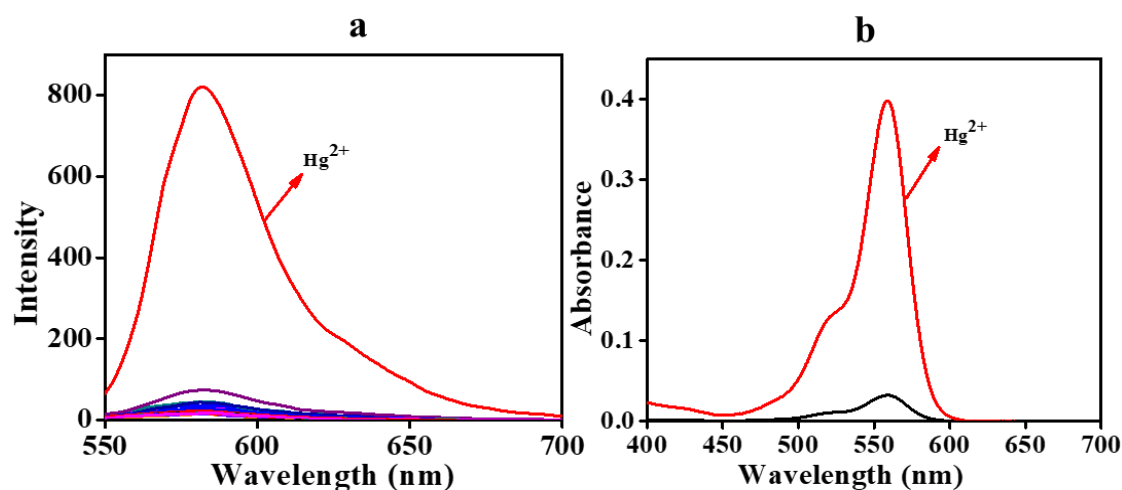

Figure 2. Selective response of S (10 μM) towards different metal cations (10 μM) (a) fluorescence at 583 nm and (b) absorption at 558 nm, respectively.
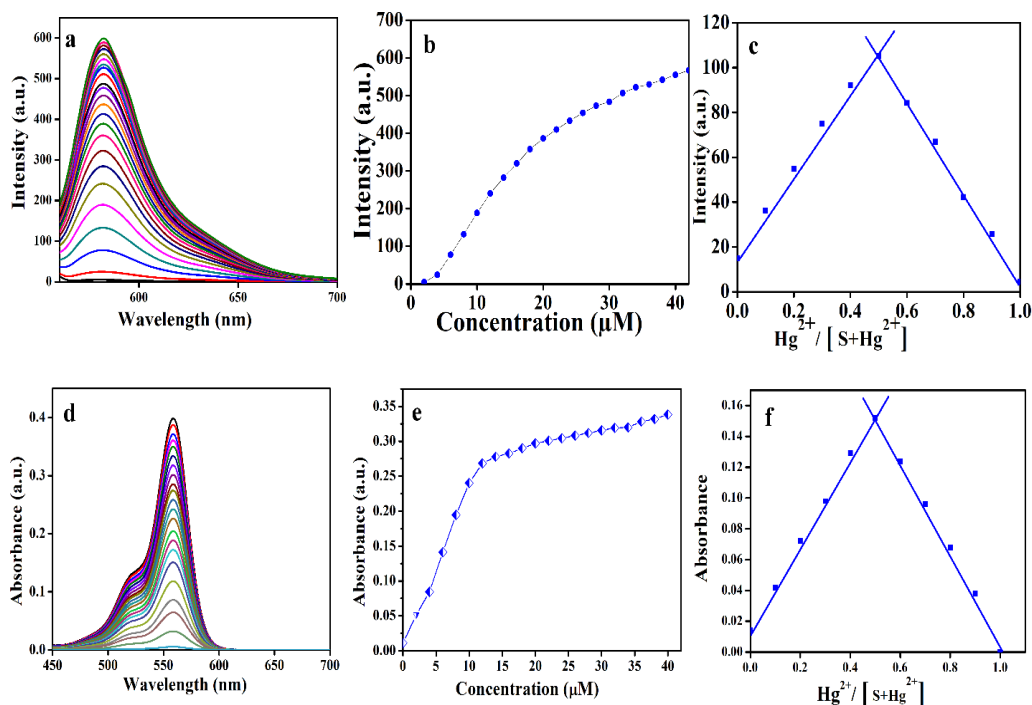
Figure 3. Titration data (emission and absorbance a and d) of S (10 μM) in response to the varying concentration of Hg^{2+} (0–40 μM) (b, e) Emission and absorption intensity (d, f) Job's plot to calculate binding stoichiometry.

3.2. Detection limit

The lower limit of detection (LOD) was calculated with the slope of linear fit obtained from the emission and absorption intensity data (Figure 4a and 4b). Equation 3 was used to calculate the LOD by fitting the linear fit data (inset Figure 5a and 5b) into the equation. The calculated value was as low as 6.9 μM.
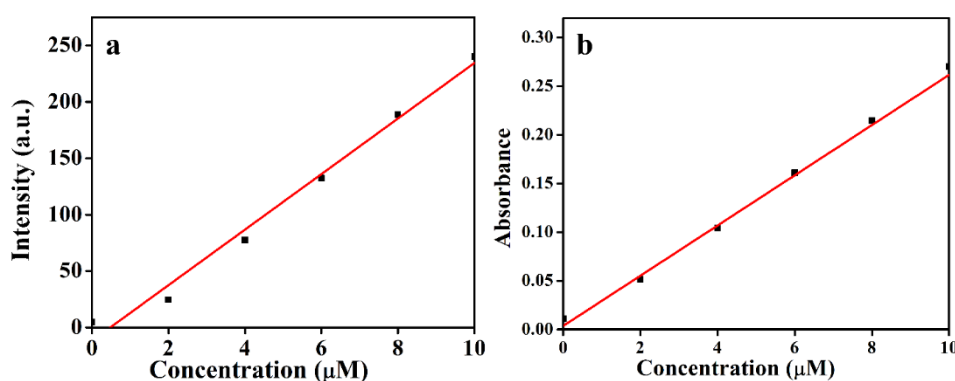
$$LOD = 3SD/ Slope \qquad (3)$$

Figure 4. Linear fit obtained from the (a) emission and (b) absorption intensity data to calculate LOD.
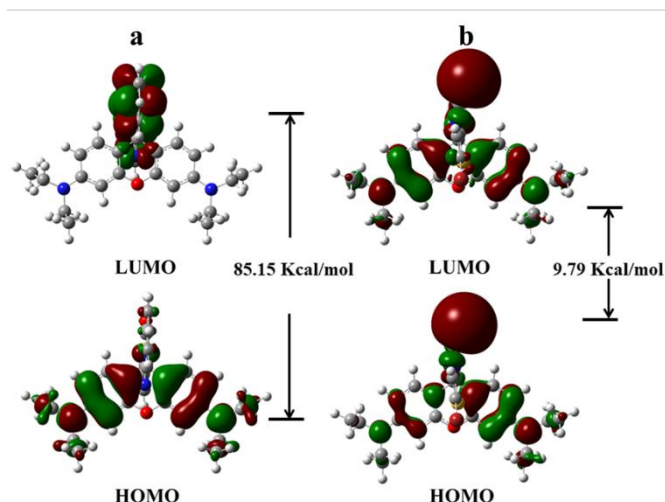
Figure 5. Frontier molecular orbitals and electron density distributions of (a) S (b) S-Hg^{2+}.

3.3. Proposed binding mechanism

Computational study of the probe S and S-metal ion complex was carried out to gain an insight into the coordination of Hg^{2+} with a chemical sensor and the resulting colorimetric changes. The density functional theory (DFT) method along with the hybrid-generalized gradient approximation (HGGA) functional B3LYP was used to optimize the ground-state structures of sensor S and S-based complexes. A Gaussian09 program package was employed to record all the calculations. The orbital energies and spatial distributions of HOMO and LUMO of S and S-Hg^{2+} were also calculated and it can be seen in Figure 5a and 5b that the π electronic cloud of HOMO of S-Hg^{2+} is located on the imide carbonyl group of rhodamine moiety, while most of the LUMO orbitals are positioned at center of the analyte (Hg^{2+}). Furthermore, as compared to the S, the energy gap between the HOMO-LUMO of S-Hg^{2+} becomes smaller.

Meanwhile, the HOMO−LUMO energy gap of the complex becomes much smaller relative to that of probe S. The energy gaps between HOMO and LUMO in the probe S and S-Hg^{2+} complex were 85.15 and 9.79 kcal/mol, respectively. This low energy values indicate that the Hg^{2+} binds well with S through bi-coordination, and the complete complex presents a planar geometry. Further, we can conclude that these low energy complexes formed by the coordination of the oxygen atom of the carbonyl group of imide linkage and the Sulphur atom of the thiazole moiety. On the bases of these calculations, the proposed binding mechanism is shown in scheme 2.
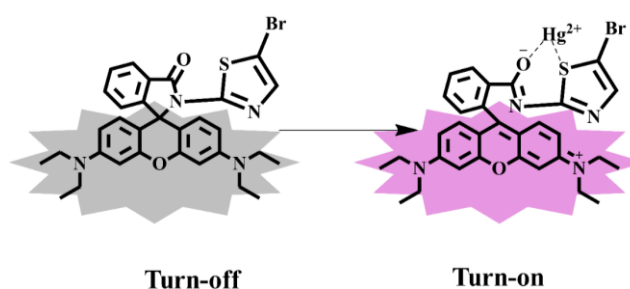
Scheme 2. Proposed binding mode of the analyte with a chemical sensor.

3.4. The selective spectral response of S-Hg^{2+} complexes against miscellaneous anions/ cations

As it is evident from the spectral investigations (emission and absorption) that the probe S selectively binds with Hg^{2+} resulting in the formation of complex S-Hg^{2+}. Another important feature of the sensor S is its reversibility and sensitivity. We have tried to explain the influence of different anions on metal-ligand complexation (turn-on) state and to generate the turn-off state of the probe S. It can be seen from the Figure 6a and 6b that adding disodium EDTA (10 μM) to the solution of S-Hg^{2+} regenerates the original spectra as in case of S. While the other anions such as F$^-$, Br$^-$, NO$_3^-$, I$^-$, SO$_4^{2-}$, CH$_3$COO$^-$ (10 μM each) etc. have no effect on the spectra obtained from S-Hg^{2+}. Hence, we can conclude that the addition of EDTA^{2-} can only generate a reversible change (fluorescent to non-fluorescent) to the solution of S-Hg^{2+}. This reversible change reveals that the complex formation is reversible in the presence of disodium EDTA. Similarly, the interference study of the competitive cations was also investigated by using the equimolar solution of different metal cations to the solution of S-Hg^{2+}. It is evident from the Figure 7a and 7b that all the interfering cations do not affect the emission and absorption intensities of the complex. Therefore, it can be concluded that the sensor S is highly sensitive and selective for Hg^{2+} only.
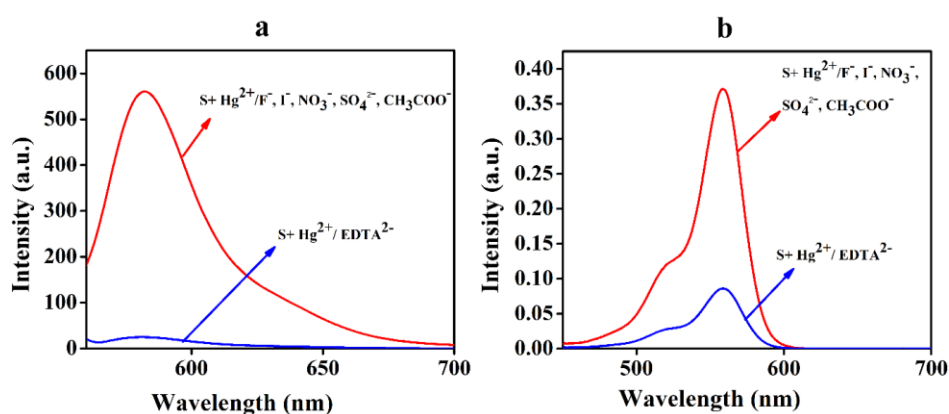

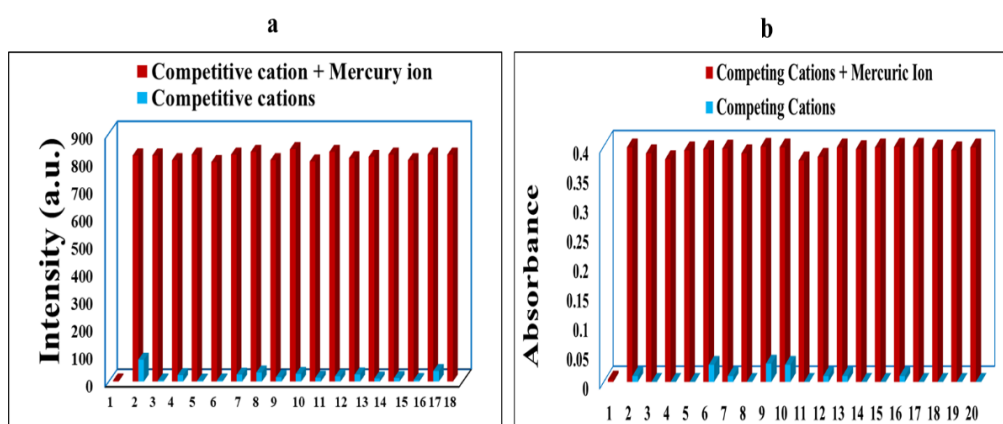**Figure 6.** Regeneration of original spectra by the interaction of EDTA^{2-}.

Figure 7. Competitive cations study of S by using equimolar concentration of competitive cations to the solution of S-Hg^{2+}.

3.5. Real-time monitoring of Hg^{2+} in the contaminated wastewater

Considering the Hg^{2+} as a toxic metal ion, the sensor S was employed to detect Hg^{2+} in the environmental wastewater collected from the river near the industrial area of Shanghai city. Then the as-prepared aliquot of this wastewater was analyzed with S followed by spiking with Hg^{2+} at different concentrations as discussed in the materials and methods section. The fluorescence intensity was measured at 583 nm and related linearly with the concentration of the analyte. For control, the same experiment was carried out with distilled water (Figure 8a and 8b). The results obtained are summarized in Table 1.
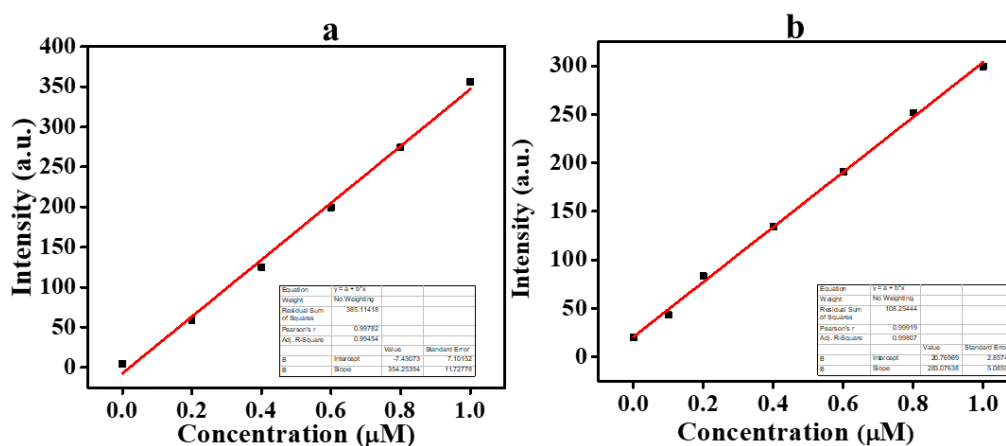

Figure 8. Linear plot of changes of fluorescence intensity of S at 583 nm versus spiked concentrations of mercury ions from 0 to 1.0 μM (a) industrial wastewater (b) distilled water.

4. Conclusions

The current study demonstrated a new type of rhodamine-assisted chemosensor for the monitoring and detection of highly toxic environmental pollutant Hg^{2+} in aqueous systems. Results evidenced that the chemical sensor displays a real-time fluorometric response with high selectivity and sensitivity to distinguish Hg^{2+} in the partial aqueous media. Both, the binding affinity and detection limit were calculated to be $4.72 \times 10^4 \, \text{M}^{-1}$ and 6.9 μM, respectively. Further, the complex between the chemical sensor and Hg^{2+} was observed to be reversible in the presence of EDTA^{2-}. Taken together, all these properties suggest that the chemo-sensor might display great potential in the field of environmental monitoring of toxic elements.

Acknowledgments

Conflict of interest

All authors declare no conflict of interest in any capacity.

References

1. M. Vendrell, D. Zhai, J. C. Er, et al., Combinatorial strategies in fluorescent probe development, *Chem. Rev.*, **112** (2012), 4391–4420.

2. S. Erdemir and O. Kocyigit, Reversible "OFF–ON" fluorescent and colorimetric sensor based benzothiazole-bisphenol A for fluoride in MeCN, *Sens. Actuat. B: Chem.*, **221** (2015), 900–905.

3. G. Hernandez-Vargas, J. E. Sosa-Hernández, S. Saldarriaga-Hernandez, et al., Electrochemical Biosensors: A solution to pollution detection with reference to environmental contaminants, *Biosensors*, **8** (2018), 29.

4. T. Rasheed, M. Bilal, F. Nabeel, et al., Fluorescent sensor based models for the detection of environmentally-related toxic heavy metals, *Sci. Total Environ.*, **615** (2018), 476–485.

5. T. Rasheed, C. Li, M. Bilal, et al., Potentially toxic elements and environmentally-related pollutants recognition using colorimetric and ratiometric fluorescent probes, *Sci. Total Environ.*, **640** (2018), 174–193.

6. L. Ling, Y. Zhao, J. Du, et al., An optical sensor for mercuric ion based on immobilization of rhodamine B derivative in PVC membrane, *Talanta*, **91** (2012), 65–71.

7. G. D. Huy, M. Zhang, P. Zuo, et al., Multiplexed analysis of silver (I) and mercury (II) ions using oligonucletide–metal nanoparticle conjugates, *Analyst*, **136** (2011), 3289–3294.

8. A. Kaur, H. Sharma, S. Kaur, et al., A counterion displacement assay with a Biginelli product: a ratiometric sensor for Hg 2^+ and the resultant complex as a sensor for Cl$^-$, *RSC Adv.*, **3** (2013), 6160–6166.

9. S. Kraithong, P. Damrongsak, K. Suwatpipat, et al., Highly Hg 2^+-sensitive and selective fluorescent sensors in aqueous solution and sensors-encapsulated polymeric membrane, *RSC Adv.*, **6** (2016), 10401–10411.

10. S. Rodriguez-Mozaz, M. J. L. de Alda, D. Barceló, Biosensors as useful tools for environmental analysis and monitoring. *Anal. Bioanal. Chem.*, **386** (2006), 1025–1041.

11. D. Barceló and P. D. Hansen, Biosensors for the environmental monitoring of aquatic systems, In: Bioanalytical and chemical methods for endocrine disruptors, **5** (2008).

12. M. Taki, K. Akaoka, S. Iyoshi, et al., Rosamine-based fluorescent sensor with femtomolar affinity for the reversible detection of a mercury ion, *Inorg. Chem.*, **51** (2012), 13075–13077.

13. M. Farré and D. Barceló, Toxicity testing of wastewater and sewage sludge by biosensors, bioassays and chemical analysis, *TrAC Trends Anal. Chem.*, **22** (2003), 299–310.

14. T. Rasheed, C. Li, F. Nabeel, et al., Self-assembly of alternating copolymer vesicles for the highly selective, sensitive and visual detection and quantification of aqueous Hg^{2+}, *Chem. Eng. J.*, **358** (2019), 101–109.

15. L. Xu, M. L. He, H. B. Yang, et al., A simple fluorescent probe for Cd^{2+} in aqueous solution with high selectivity and sensitivity, *Dalt. Transact.*, **42** (2013), 8218–8222.

16. C. Bosch-Orea, M. Farré and D. Barceló, Biosensors and bioassays for environmental monitoring. In: Past, present and future challenges of biosensors and bioanalytical tools in analytical chemistry: A tribute to Professor Marco Mascini, *Comprehen. Anal. Chem.*, **77** (2017), 337–373.

17. E. M. Nolan and S. J. Lippard, Tools and tactics for the optical detection of mercuric ion, *Chem. Rev.*, **108** (2008), 3443–3480.

18. C. M. Carvalho, E. H. Chew, S. I. Hashemy, et al., Inhibition of the human thioredoxin system a molecular mechanism of mercury toxicity, *J. Biol. Chem.*, **283** (2008), 11913–11923.

19. J. Wang and X. Qian, A series of polyamide receptor based PET fluorescent sensor molecules: positively cooperative Hg^{2+} ion binding with high sensitivity, *Org. Lett.*, **8** (2006), 3721–3724.

20. K. A. Merritt and A. Amirbahman, Mercury methylation dynamics in estuarine and coastal marine environments—A critical review, *Earth-Sci. Rev.*, **96** (2009), 54–66.

21. T. Zhang, B. Kim, C. Levard, et al., Methylation of mercury by bacteria exposed to dissolved, nanoparticulate, and microparticulate mercuric sulfides, *Environ. Sci. Technol.*, **46** (2012), 6950–6958.

22. World Health Organization, Guidelines for drinking-water quality, 3rd Ed., Vol. 1, Geneva, 2004.

23. T. Rasheed, C. Li, Y. Zhang, et al., Rhodamine-based multianalyte colorimetric probe with potentialities as on-site assay kit and in biological systems, *Sens. Actuators. B.*, **258** (2018), 115–124.

24. T. Rasheed, C. Li, L. Fu, et al., Development and characterization of newly engineered chemosensor with intracellular monitoring potentialities and lowest detection of toxic elements, *J. Mol. Liq.*, **272** (2018), 440–449.

25. Y. Cao, L. Ding, W. Hu, et al., Selective sensing of copper and mercury ions with pyrene-functionalized fluorescent film sensor containing a hydrophilic spacer, *Appl. Surf. Sci.*, **273** (2013), 542–548.

26. N. Wanichacheva, N. Prapawattanapol, V. S. Lee, et al., Hg^{2+}-induced self-assembly of a naphthalimide derivative by selective "turn-on" monomer/excimer emissions, *J. Luminesce.*, **134** (2013), 686–690.

27. X. Chen, T. Pradhan, F. Wang, et al., Fluorescent chemosensors based on spiroring-opening of xanthenes and related derivatives, *Chem. Rev.*, **112** (2011), 1910–1956.

28. W. Zhu, X. Chai, B. Wang, et al., Spiroboronate Si-rhodamine as a near-infrared probe for imaging lysosomes based on the reversible ring-opening process, *Chem. Commun.*, **51** (2015), 9608–9611.

29. X. Zhang and Y. Y. Zhu, A new fluorescent chemodosimeter for Hg^{2+}-selective detection in aqueous solution based on Hg^{2+}-promoted hydrolysis of rhodamine-glyoxylic acid conjugate, *Sens. Actuat. B: Chem.*, **202** (2014), 609–614.

30. Y. Yuan, S. Sun, S. Liu, et al., Highly sensitive and selective turn-on fluorescent probes for Cu^{2+} based on rhodamine B, *J. Mater. Chem. B.*, **3** (2015), 5261–5265.

31. W. Zhao, X. Liu, H. Lv, et al., A phenothiazine–rhodamine ratiometric fluorescent probe for Hg^{2+} based on FRET and ICT, *Tetrahedr. Lett.*, **56** (2015), 4293–4298.

32. M. H. Lee, J. S. Wu, J. W. Lee, et al., Highly sensitive and selective chemosensor for Hg^{2+} based on the rhodamine fluorophore, *Org. Lett.*, **9** (2007), 2501–2504.

33. J. Y. Kwon, Y. J. Jang, Y. J. Lee, et al., A highly selective fluorescent chemosensor for Pb^{2+}, *J. Am. Chem. Soc.*, **127** (2005), 10107–10111.

34. H. Lu, S. S. Zhang, H. Z. Liu, et al., Experimentation and theoretic calculation of a bodipy sensor based on photoinduced electron transfer for ions detection, *J. Phy. Chem. A.*, **113** (2009), 14081–14086.

35. M. J. Frisch, G. W. Trucks, H. B. Schlegel, et al., Gaussian 09, Inc., Wallingford CT, USA, (2013).